



Shahrood University of
Technology



Iranian Society of
Mining Engineering
(IRSM)

Assessment of Discontinuities-Induced Overbreak by Tunnel Advancement using Discrete Fracture Network (Case study: Alborz Tunnel, Iran)

Mohammad Amin Hajimohammadi¹, Mojtaba Bahaaddini^{1*}, Mohammad Hossein Khosravi², Hassan Vandyoosefi³

1. School of Mining Engineering, College of Engineering, University of Tehran, Tehran, Iran

2. Department of Mining Engineering, Faculty of Engineering, University of Birjand, Birjand, Iran

3. Geotechnical Engineering Department, General Mechanics Co., Tehran, Iran

Article Info

Received 17 December 2025

Received in Revised form 24
February 2025

Accepted 10 April 2025

Published online 10 April 2025

DOI: [10.22044/jme.2025.15465.2966](https://doi.org/10.22044/jme.2025.15465.2966)

Keywords

Discrete fracture network

Tunnel advancement

Overbreak

Kinematic stability analysis

Alborz tunnel

Abstract

Discontinuities are known as a primary factor in instability of tunnels and underground excavations. To prevent potential damage and overbreak by underground advancement, it is essential to provide a model, which considers both the geometrical and mechanical characteristics of discontinuities. Discrete Fracture Network (DFN) is a conceptual model to represent and analyse the complex system of discontinuities within the rock mass. Combined DFN with analytical or numerical methods can be employed as a scientific tool to analyse generated rock blocks, and their stabilities under different loading conditions. This paper aims to investigate the created overbreak by tunnel advancement in the Alborz tunnel located in the Tehran-North freeway in Iran. First, the geometrical characteristics of discontinuities were surveyed by tunnel advancement in 200 meters. Four major joint sets and a bedding plane were identified and their statistical characteristics were measured. The DFN model was generated and its validity was investigated through a comparison against field data. The average volume of generated blocks in the studied area was measured 0.22 m³. The stability of generated blocks around the opening was kinematically evaluated. The volume of formed blocks around tunnel in the DFN model prone to instability due to static or dynamic loads was estimated 2605 m³ while the measured overbreak in field was 2735 m³. The depth of overbreak in DFN model showed a good agreement with field measurements. The results show that DFN model combined with kinematic stability analysis can provide a scientific tool to investigate geological overbreak in underground excavations.

1. Introduction

Rock mass is known as a complex geomaterial due to its heterogenous and anisotropic nature. Rock engineers are commonly encountered with several challenging questions in the design of structures within the rock mass. Various failure modes may occur in a rock mass, which depend on numerous factors such as its geomechanical characteristics, stress state, groundwater condition, and excavation dimensions [1]. Discontinuities play a crucial role in the strength and deformation of the rock mass [2, 3]. Rock mass behavior under different stress states and strain conditions depends on the nature and properties of discontinuities.

These properties include orientation, surface roughness, length, persistence, spacing, filling, and fracture termination. The orientation of joints is also a crucial feature, which dictates the potential movement of a rock mass and the corresponding volume of unstable material [1, 4].

Construction of tunnels within jointed rock masses is often accompanied by challenges such as overbreak, which refers to the excavation of material beyond the intended tunnel profile. The overbreak can impact underground constructions with increased cost of support systems, slow advancement rate, and higher post-construction



maintenance cost and possible water seepage through unfilled voids at the lining extrados [5]. Overbreak not only increases construction costs and time, but also poses significant risks to the stability and safety of the tunnel. The occurrence of overbreak is closely linked to the presence and characteristics of discontinuities within the rock mass. Discontinuities act as planes of weakness, influencing stress redistribution, and failure mechanisms during tunnel advancement [6, 7].

The prediction of overbreak during excavation is a challenging task in tunnelling and mining projects. As schematically shown in Figure 1, the overbreak can be divided into two main categories; namely geological overbreak, caused by geomechanical features of the rock mass, and

technical overbreak, related to drill-and-blast design and execution. Overbreak refers to the volume of the rock mass excavated beyond the designed specifications, while underbreak represents the rock volume left within the desired tunnel space. The former scenario occurs more frequently than the latter [8]. Drill-and-blast excavations are still widely used in mining, quarrying and hard rock tunnelling due to its relatively low costs and simplicity of the implementation [5]. However, this method has the inherent disadvantage of damaging the surrounding rock mass around the excavated section and possibly development of blast-induced undesired cavities.

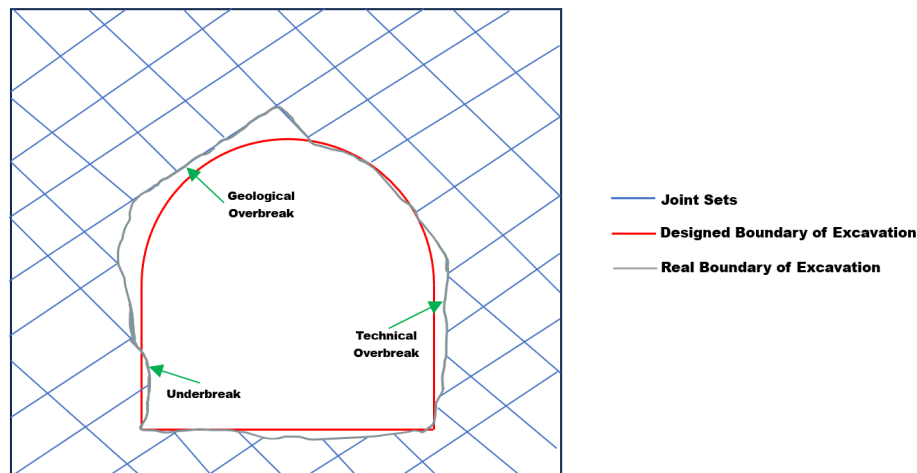


Figure 1. Schematic illustration of the theoretical and actual tunnel profiles, highlighting the geological induces overbreak.

The geological overbreak can be hardly avoided, and it may be predicted by investigating the rock mass characteristics. However, the technical overbreak can be controlled by adopting appropriate blasting or excavation techniques [6]. The precise prediction of overbreak extent and the associated technical and economic impacts, are challenging in hard rock tunnelling projects.

The additional costs associated with overbreak often become a common subject of dispute between clients and construction companies. In tunnelling projects, certain regulations are commonly implemented to evaluate the economic impact of the overbreak, attempting to distinguish between geological overbreak (typically covered by the client) and technical overbreak (often attributed to the construction company). Construction tolerance is generally considered between the design and excavation phases. This

tolerance indicates the allowable deviation between the design and actual excavation volumes [8].

A limited number of studies has been undertaken to develop an analytical model for estimation of the overbreak. Mahtab et al. [9] proposed an analytical approach to assess admissible thresholds of the geological overbreak with a given level of confidence, considering the uncertainty in main rock mass characteristics. This approach is based on the two-dimensional limit equilibrium analysis of rock wedges at the perimeter of the excavation calculated on the basis of the stress field around a circular hole in an anisotropic elastic medium. Mohammadi et al. [10] tried to determine the effect of longwall working on the extension damage zone above main gate roadway. Due to complex nature of the rock mass and associated difficulties in analytical description

of the rock mass, these studies are very limited and rarely can describe the real scenarios.

The common approaches to assessing overbreak rely on empirical methods, machine learning techniques or continuum-based numerical models, which often oversimplify the complex nature of fractured rock masses. These methods may fail to capture the intricate interactions between discontinuities and their impact on rock behaviour during excavation [11].

Singh and Xavier [12] by undertaking small scale blasting in physical models and the assessing the associated blast damage, highlighted that the improper blast design can intensify overbreak in drill-and-blast tunnelling. Khalili et al. [13] using numerical Finite Element Method (FEM) tried to estimate the effect of blast pattern on damage and post-failure zone occurred around the Miyaneh-Ardabil railway tunnel. However, Farrokhi et al. [14] declared that the mechanized excavation does not eliminate overbreak but shifts its causes to machine-rock interaction issues.

Innaurato et al. [15] and Schmitz et al. [16] attempted to correlate the rock mass quality, quantified in terms of Rock Mass Rating (RMR) and Rock Quality Designation (RQD) indexes, and the overbreak volume measured by topographic surveys. Dey and Murthy [17] developed a composite blast-induced rock damage predictive model, considering rock mass parameters, blast design parameters, and explosive charge parameters, where their model was validated with laboratory and field investigations at five tunnels. Gong et al. [18] applied a statistical approach, based on the Bayes discriminant analysis, for prediction of overbreak and its discriminant factors. Eight parameters; including four orientation parameters of the two dominant joint sets (dip and dip direction of joint sets), two orientation parameters of the excavation surface (dip and dip direction), the extension and spacing of discontinuities, were adopted as geometric parameters influencing the over-excavation. Jang and Topal [19] tried to predict overbreak using ANN, linear and nonlinear regressions between geomechanical characteristics (UCS, RQD, RMR, joint spacing, orientation and joint conditions) with the measured overbreak. Daraei and Zareh [20] tried to simulate the the excavation damage zone around tunnel boundary and estimated the overbreak depth by the rock strength factor. Mottahedi et al. [21] by investigating 270 datasets from drill and blast tunnels tried to develop adaptive neuro-fuzzy inference system and particle swarm optimization model to estimate the

overbreak. However, review of these studies clearly shows that the assessment of discontinuities induced overbreak has been remained a challenge in empirical, numerical and machine learning techniques due to associated difficulties in providing the structural geological model.

In recent years, the Discrete Fracture Network (DFN) approach has emerged as a powerful tool for explicitly representing the geometry, distribution, and connectivity of discontinuities in rock masses. By incorporating stochastic or deterministic fracture properties, DFN models provide a more realistic representation of the rock mass, enabling detailed analysis of fracture-induced phenomena such as overbreak [22, 23].

DFN is a three-dimensional geometric representation of joints within a rock mass. Nowadays, DFN modelling has found a wide range of application in mining and civil engineering projects. Dershowitz and Herda [24] by considering the finite size of discontinuities, developed a 3D stochastic simulation procedure to generate a DFN model. Staub et al. [25] criticized the use of DFN modelling in stability analysis due to limitations of tunnel mapping and unknown size and shape of fracture inside the rock mass. Hadjigeorgiou [26] evaluated DFN models validity based on data acquisition which is the subject of calibration and validation. Elmo et al. [27] investigated the ability of the DFN models for estimation of the equivalent rock mass properties for continuum modelling and showed that this approach can improve the predictability of the geomechanical simulations and the empirical rock mass classification systems. Noroozi et al. [28] developed a code, namely DFN-FRAC3D, to describe damage zones around the strike-slip faults. Elmo et al. [29] provided guidelines for the quantitative description of discontinuities for the use in DFN modelling. Grenon et al. [30] employed DFN modelling to study the structurally-defined rock blocks, such as wedges created around excavations. They declared that there is a greater demand to review the process of fracture data collection for DFN modelling. Noroozi et al. [31] developed a coupled DFN-FEM model to assess the stability of support systems in a diversion tunnel at the Rudbar Lorestan dam site. Vaziri et al. [32] investigates the effect of geometrical parameters of non-persistent joints on the mechanical behaviour of the rock masses using combined DEM and DFN. Ghaedi Ghalini et al. [33] employed DFN modelling approach to estimate the in-situ block size distribution for analysing rock blocks fragmentation after blasting.

Measurement of the rock mass structural properties is not feasible at three-dimension and these properties are commonly measured through surface exposures or linear surveys. The standard process in generation of a DFN model involves defining fracture properties, which are noted in Table 1. The primary properties include geometrical parameters for generation of a DFN model while the secondary properties may also be

defined, depending on the model application for hydraulic or geomechanical studies. The validity of a DFN model is commonly achieved by comparing the direction, intensity, and pattern of simulated fracture traces with the measured field data. The stochastic approach offers the best option for creating realistic geometrical models of discontinuities [29].

Table 1. Primary and secondary properties for defining a DFN model [34].

Primary	Secondary
Orientation distribution	Aperture distribution
Fracture length distribution	Fracture shear strength properties
Fracture intensity distribution	Fracture stiffness properties
Spatial variation of fracture intensity	Fracture transmissivity distribution
	Storativity distribution
	Termination percentage

This work aims to study the induced geomechanical overbreak using the DFN modelling for the Alborz tunnel located in section II of Tehran-North freeway in Iran. The geometrical characteristics of discontinuities for 200 m of this tunnel were surveyed and the statistical distribution functions for the orientation and the trace length were determined. The fracture intensity was measured by the the tunnel advancement in the studied zone. Then, the DFN model was generated for the studied area and its validity was evaluated based on the field measurement. By undertaking a kinematic stability analysis based on the block weight and the shear strength of rock joints, unstable blocks were determined and the amount of geological overbreak was measured in the DFN model. The estimated overbreak was then compared with field measurement. The presented methodology in this study can be employed as a useful and scientific tool for measurement of geomechanical overbreak in underground excavations.

2. Case study (Alborz Tunnel)

Alborz tunnel is located in the second part of Tehran-North freeway and is known as the longest road tunnel in Iran with a length of more than 6 km. The tunnel cross-section is horseshoe-shaped, with a width of 12.6 meters. This tunnel is located in the Alborz Mountain ranges and inside the geological formations of Shamshek and Karaj. The lithology along the tunnel axis consists mostly of tuffs

(black, green, grey), andesite (green and grey), anhydrite, limestone, sandstone, argillite, and gabbro, as shown in Figure 2. The excavation method was controlled blasting in two sections; the semi-circular excavation of top part followed by the installation of primary support and the excavation of the bench section. This studied area in this research located at 1,600 to 1,800 meters from the northern entrance of the tunnel (see Figure 3).

In the studied area, tunnel passes through sedimentary rocks of the Shemshak formation, where the lithology of the encompassing rock is predominantly sandstone and argillite (sandstone for 1,600 to 1,617 meters, sandstone with argillite layers for 1,617 to 1,730 meters, argillite for 1,730 to 1,748 meters and alternating layers of argillite and sandstone for 1,748 to 1,800 meters). Twenty-four faults are located in the studied area. The excavation of this section has been a challenge for geotechnical engineers due to intense tectonics and the presence of argillite layers accompanied by geological instabilities. The uniaxial compressive strength (UCS) of the sandstone and argillite rocks in this section vary in the range of 70-100 MPa and 25-50, respectively [35]. Overbreak at various tunnel cross-sections have been documented in the studied area. A typical record of overbreak is illustrated in Figure 4. The volumetric percentage of overbreak lies within the range of 8.58 to 18.94% of the tunnel volume.

statistical properties of joint sets were determined based on the Fisher distribution function. The Fisher distribution defines a symmetrical angular distribution of orientations about the mean orientation vector. The probability density function of Fisher can be expressed as follows,

$$f(\theta) = \frac{\theta \sin \theta e^{\kappa \cos \theta}}{e^{\kappa} - e^{-\kappa}} \tag{1}$$

where θ is the angular deviation from the mean vector, and κ is the Fisher dispersion coefficient. The statistical orientation of joint sets is expressed using dip, dip direction, and κ , which are summarised in Table 2.

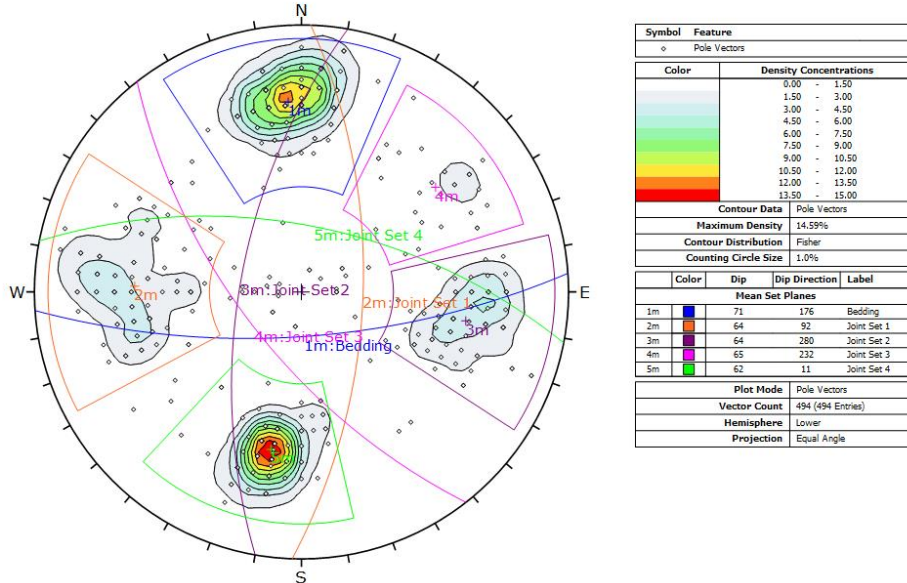


Figure 5. The identified joint sets based on orientation clustering of the filed surveys.

Table 2. Fisher statistical distribution parameters for the joint orientation.

Joint set ID	Statistical properties of joint sets		
	Dip (degrees)	Dip direction (degrees)	Fisher's constant (κ)
bedding	71	176	58.06
1	64	92	24.47
2	64	280	35.16
3	65	232	28.31
4	62	11	60.74

3.2. Fracture size

The fracture size is an important parameter in DFN models which is commonly determined through the measurement of the trace length. The trace length can only be collected by exposing the rock mass. For each trace intersects the tunnel surface, the trace length was recorded. A statistical distribution should be compatible with the trace length data as they will be compared with the simulated trace lengths [38]. In many cases, fracture lengths are reported as the diameter of the fractures or the radius of the fractures. The size of the fractures may follow exponential, power or log-normal distributions [39, 40].

In this study, the distribution function of the fracture lengths was determined based on Kolmogorov–Smirnov, Anderson-Darling and Chi-square tests where the best distribution was selected based on the lowest root mean square error (RMSE). Joint sets 1, 2 and 4 showed log-normal distributions, while joint set 3 exhibited an exponential distribution, as shown in Figure 6. The statistical parameters of these sets are summarised in Table 3. As the bedding plane was considered deterministic in DFN simulations which was defined based on the measured spacing, it was disregarded for statistical analyses.

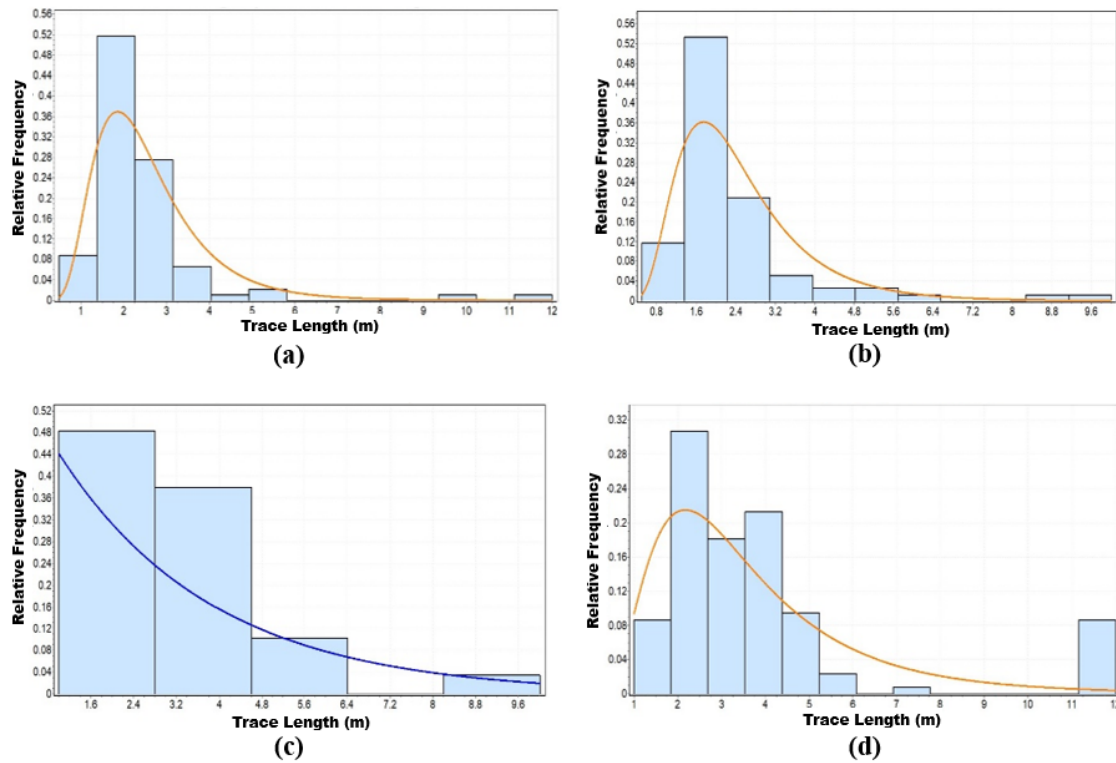


Figure 6. Statistical distributions of the fracture trace length: a) Joint set 1, b) Joint set 2, c) Joint set 3 and d) Joint set 4.

Table 3. Statistical characteristics of the fracture size.

Joint set ID	Statistical distribution	Standard deviation	Median μ (m)
1	Lognormal	0.46	0.83
2	Lognormal	0.79	0.48
4	Lognormal	0.60	1.13
3	Exponential	----	$\lambda = 0.35$

3.3. Fracture intensity

The fracture density is commonly measured by counting the frequency of fracture traces along scanlines (i.e. the number of fractures per meter) using a fixed distance, usually in the range of 2-5 meters. Dershowitz and Herda [24] suggested a system for describing the fracture intensity based on the sampling region dimension and the feature dimension. In this system, P is written with two subscripts, which refer to the dimension of the sampling area and the fracture dimension, respectively. These subscripts include 0, 1, 2, 3, which refer to number, line, area, and volume, respectively. The common approach for measurement of the fracture intensity is based on P_{10} (fracture frequency; number of fractures per unit length) or P_{21} (summation of trace lengths in a specific area) which are both directional dependent. P_{32} is usually used for generation of DFN models which is estimated indirectly rather than being measured [38]. There is a relative

correlation between P_{10} , P_{21} , and P_{32} , where P_{32} can be estimated with random DFN simulations using the following procedure [24]:

- A value is assumed for P_{32} , called $P_{32 Mod}$, and a DFN model is simulated.
- Artificial scanlines or exposures with identical directions and sizes of the surveyed ones are created in the DFN model.
- The fracture intensity for the sampled scanlines $P_{10 Mod}$ or the surface exposures $P_{21 Mod}$ is measured in the DFN model.
- P_{32} is calculated using the relative relationship as follows,

$$\frac{P_{10 Field}}{P_{10 Mod}} = \frac{P_{21 Field}}{P_{21 Mod}} = \frac{P_{32}}{P_{32 Mod}} \quad (2)$$

The fracture intensity in this study was measured based on scanlines P_{10} and the corresponding P_{32} was calculated using Equation 2. The compositing length plays a critical role in

evaluating P_{10} for DFN modelling. An optimal compositing length should balance the need to capture geological heterogeneity and scale dependency while minimizing bias and noise. If the compositing length is too long, it may average out high-intensity zones, leading to an underestimation of fracture intensity in those areas. However, short compositing length may result in overemphasize small-scale variations, leading to an overestimation of fracture intensity in some intervals. As the fracture intensity (P_{10}) is scale-dependent, the compositing length was aligned with the scale of the problem being studied (tunnel scale) [24, 41]. The measured field fracture intensity and the calculated P_{32} for different joint sets are summarised in Table 4.

4. DFN Model Generation and Validation

The undertaken workflow for evaluation of excavation induced blocks and stability analysis is shown schematically in Figure 7. The process starts

with the data analysis and resources introduced in the previous section which are then aligned with a structural model, followed by geomechanical and engineering analyses [42]. The Baecher model [43], commonly known as the random disk model [38] was used in this work to simulate the spatial distribution of joints in the model. The process of model generation is shown in Figure 8. The geometrical properties of four joint sets described in previous section, were used as input parameters for generation of the DFN model. In this study, the faults and bedding planes were considered deterministically and the three-dimensional DFN model was generated.

Table 4. Fracture intensity for joint sets.

Joint set ID	Fracture intensity (1/m)	
	P_{10}	P_{32}
1	2.56	6.3
2	2.35	5.635
3	2.513	6.3
4	2.494	5.345

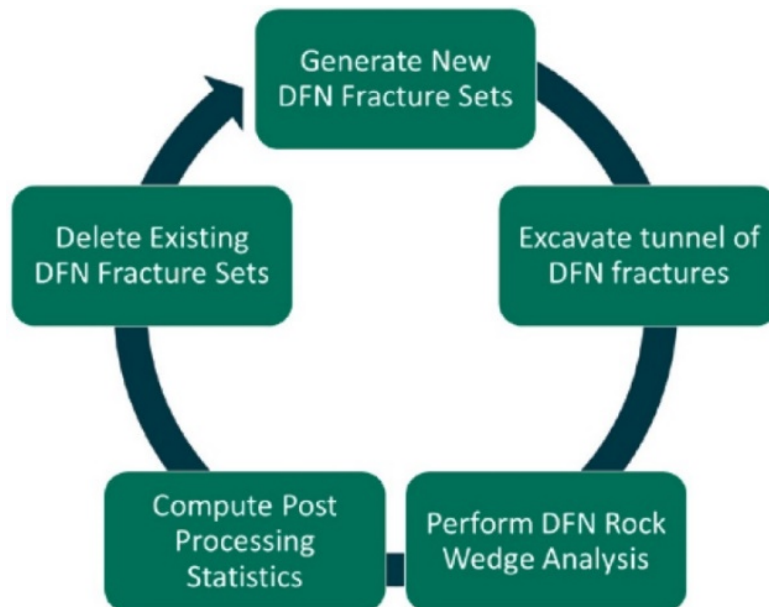


Figure 7. Workflow for the kinematic stability analysis of the DFN model [42].

To investigate the validity of the generated DFN model, the orientation distributions of generated fractures were compared with the field measurements, as illustrated in Figure 9. The results show that the orientation and distribution of joint sets are in good agreement with field measurements. The cumulative distributions of fracture trace length for all joint sets in the DFN model were also compared against field

measurements, as shown in Figure 10. For all joint sets, good agreement was found between field measurements and the generated DFN model. Furthermore, the fracture intensity of joint sets within the model were also compared against field measurements and the results are presented in Table 5. These results clearly show that the generated DFN model well represents joint system of the studied area.

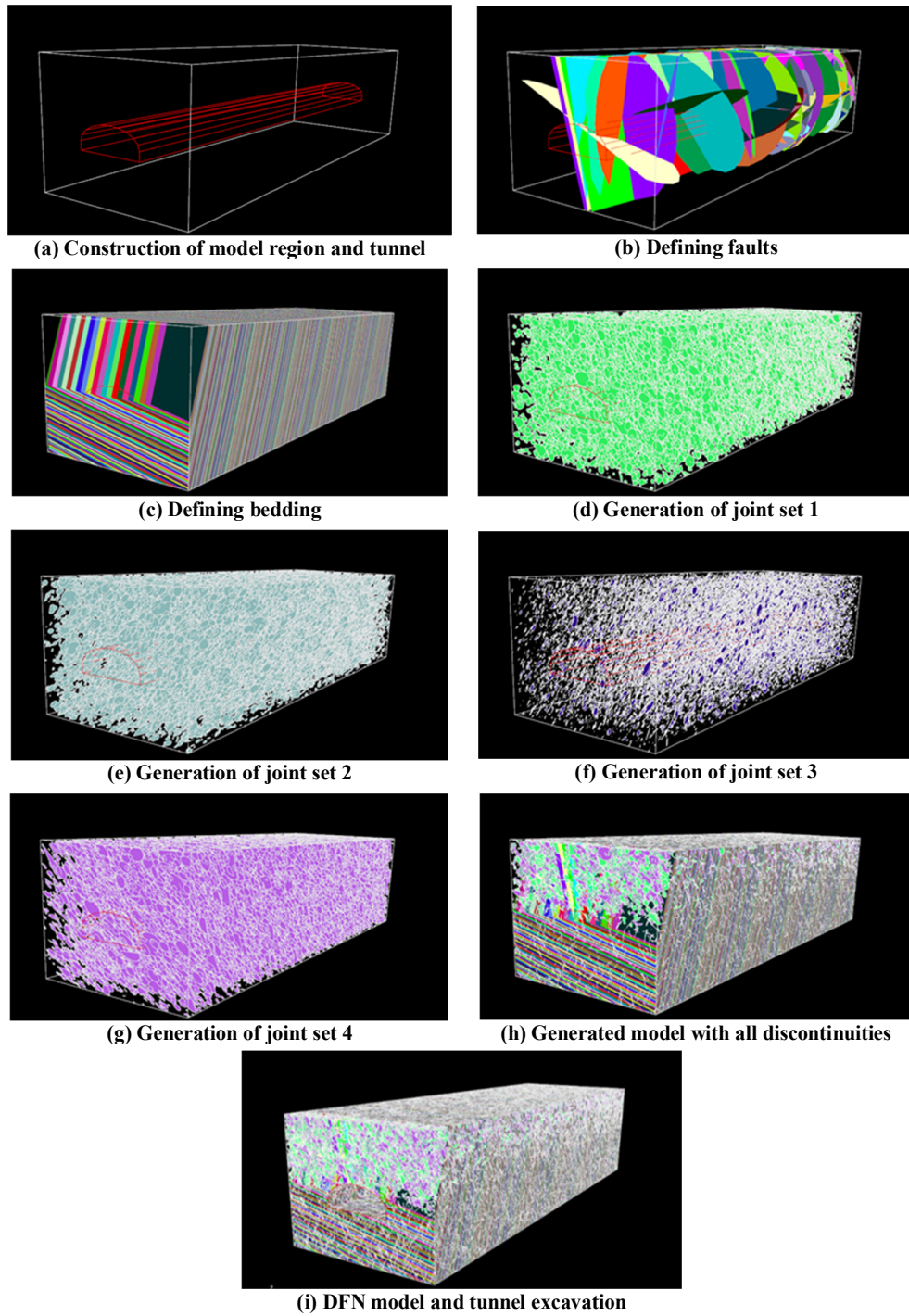


Figure 8. The process of DFN model generation of the studied area.

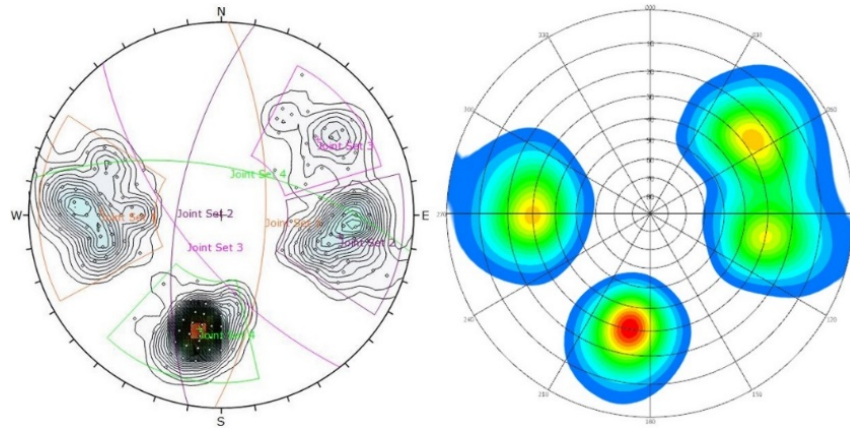


Figure 9. Comparison of the orientation and distribution of joint sets in DFN model and field measurements; (a) Field measurement and (b) Generated DFN model.

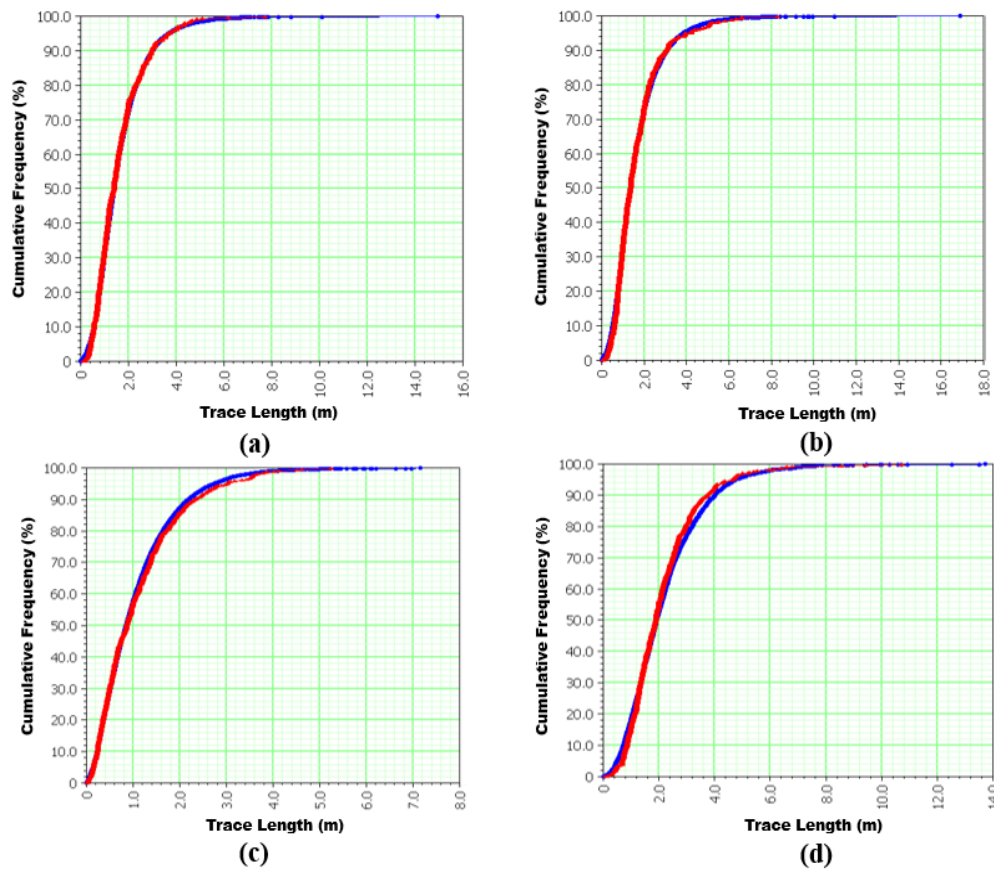


Figure 10. Comparison of the trace length in the generated DFN model (red line) and field measurements (blue line) for: a) Joint set 1, b) Joint set 2, c) Joint set 3, d) Joint set 4.

Table 5. Comparison of the fracture intensity between field measurement and model.

Joint Set ID	P ₁₀ Field	P ₁₀ Model
1	2.56	2.59
2	2.35	2.36
3	2.51	2.86
4	2.49	2.42

The block size distribution was determined in this work using the Multi-Dimensional Spacing

(MDS) method. In this approach, several points are randomly selected in the simulated DFN model and

lines in three specified directions are generated from each point. The intersection location of fractures for each line is then recorded. Then, the spacing frequency is recorded in three directions using the corresponding lengths between fractures. Finally, the block volume distribution is calculated by multiplying the spacing probability distributions using the Monte Carlo simulation method [33]. The size distribution of blocks in the generated DFN model is shown in Figure 11. The average block size (D_{50}) was measured 0.22 m^3 .

5. Tunnel Kinematic Stability Analysis

5.1. Reducing the model size

The generated DFN model, explained in previous section, has a size of $63 \times 200 \times 48.8 \text{ m}^3$. Undertaking the kinematic stability analysis in this size is computationally intensive and inefficient, if it is achievable, due to size and number of generated blocks. Therefore, reduction in the size

of DFN model compared to the tunnel scale is necessary to expedite the kinematic stability analysis of the tunnel. Therefore, the DFN model was trimmed into a region size of $37.8 \times 200 \times 29.28 \text{ m}^3$, as shown in Figure 12.

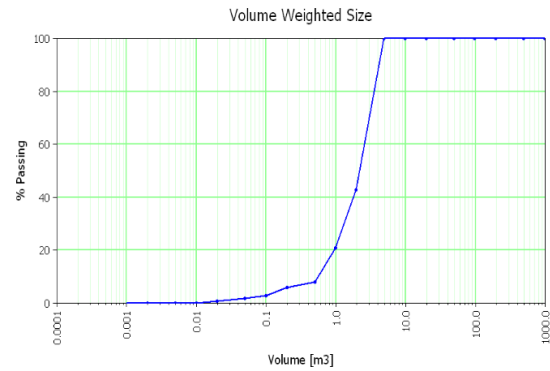


Figure 11. The block size distribution using the DFN model.

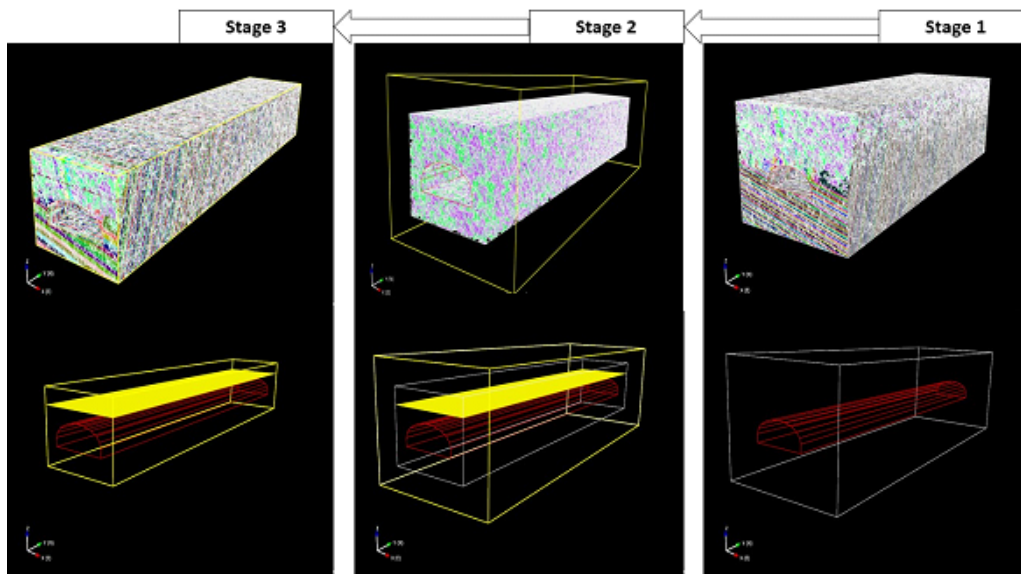


Figure 12. The procedure of reducing the model size.

A trace plane was considered at eight meters above the tunnel as shown in Figure 13 and the trace-map statistics for full and reduced sized models are presented in Table 6. It is evident that the DFN models in both full and reduced regions can be well compared according to the trace-plane statistics. This means that the DFN model is not sensitive to the size in the studied area; therefore, it

can be reduced in size. Due to highly fractured zone of this study and the long process of calculation for generated wedges around the tunnel in kinematic stability analysis, the analysed 200 m long tunnel was divided into eight zones with the optimal length of 25 m. By combining the results from these sections together, the stability analysis of 200 m from the tunnel was examined.

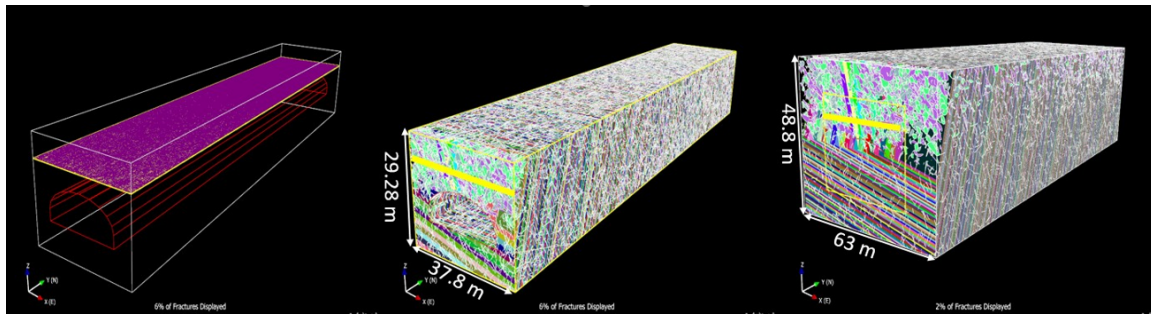


Figure 13. Comparison of the trace-plane of the DFN model ($63 \times 200 \times 48.8 \text{ m}^3$) with the reduced size region ($37.8 \times 200 \times 29.28 \text{ m}^3$). The Trace-plane shown by a yellow surface located at 8 meters above the tunnel.

Table 6. Trace-plane statistical comparison for the full and reduced sizes of studied regions.

Trace-plane Property	Original size ($63 \times 200 \times 48.8 \text{ m}^3$)	Reduced size ($37.8 \times 200 \times 29.28 \text{ m}^3$)
Number of Segments	1,130,093	1,135,222
Intersection Count	105,735	104,893
Intensity (P_{21}) (m/m^2)	27.36	23.31
Trace Length Mean (m)	1.95	1.68
Number of fractures / areas	13.98	13.87

5.2. Stability analysis of generated blocks

Models for rock domains were then evaluated for fracture intersections and connection maps and the specific stability assessment of rock block geometry at exposed faces of the tunnel. The kinematic stability analysis is initiated by determination of the wedge geometry using classical block theory described by Goodman and Shi [44]. Then all individual forces acting on wedges are determined, and the resultant active and passive force vectors for the wedge are then calculated. In general, active forces denotes driving forces in the calculation of the safety factor, while passive forces represent the resisting forces. The corresponding mass of each block is determined using the assigned rock density and the computed volume. As noted earlier, the rock type in the studied area is predominantly sandstone and

argillite and the average unit weight of rock in the studied area was considered $26.3 \text{ kN}/\text{m}^3$. By assignment of the in-situ stresses, the normal stress on each face of blocks was calculated. The sliding direction of the wedge is then determined and the corresponding normal forces on each wedge plane is calculated. The resisting forces on the joint plane is calculated using the Coulomb shear strength model. Then, the sliding of blocks on a single or multiple surfaces is assessed using the Coulomb criterion. The free fall of each block is also checked by its geometry. The friction angle of discontinuities was assigned 23 degrees. Finally, the factor of safety for each block can be determined. The kinematic stability analysis of the tunnel for 1600–1800 meters was carried out using eight sections with 25 meters interval. The results of analysis are shown in Figure 14 and Table 7.

Table 7. Results of the kinematic stability analysis in each 25 m interval.

Tunnel section	Total block volume [m^3]	Maximum block height [m]	Average block height [m]
1600-1625	339.51	2.37	0.14
1625-1650	317.90	2.32	0.13
1650-1675	345.70	2.73	0.14
1675-1700	327.23	2.04	0.13
1700-1725	313.03	2.48	0.13
1725-1750	313.29	2.00	0.13
1750-1775	325.72	1.97	0.13
1775-1800	322.19	2.48	0.13
1600-1800	2604.56		

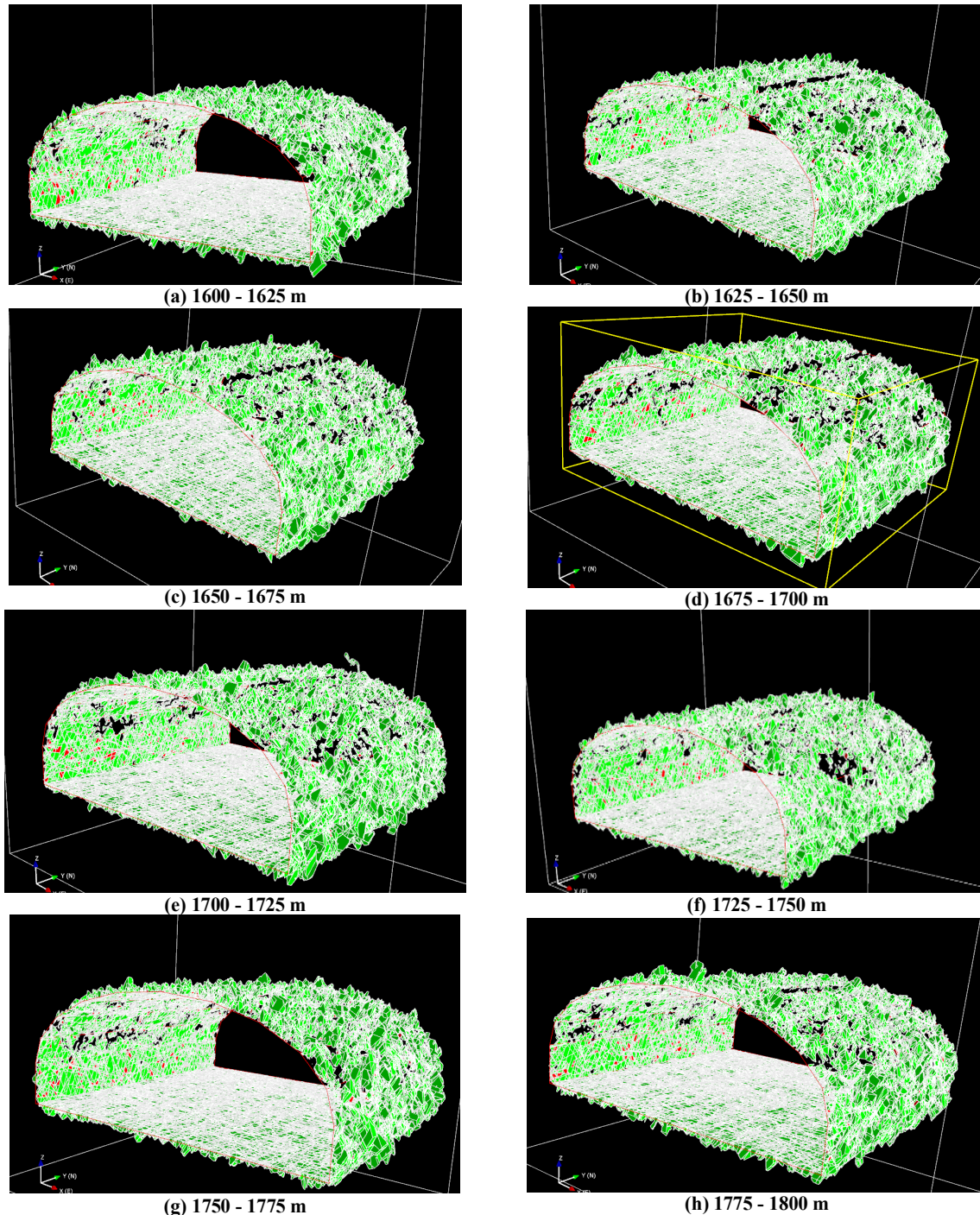


Figure 14. Kinematic stability analysis statistics for studied area: a) 1600 - 1625 m, b) 1625-1650 m, c) 1650-1675 m, d) 1675-1700, e) 1700-1725 m, f) 1725-1750 m, g) 1750-1775 m and h) 1775-1800 m.

The volume of blocks around the tunnel estimated by the DFN model was compared with the measured overbreak, and the results are presented in Figure 15. It can be observed that all the blocks formed around the tunnel collapse, which is due to the extremely high level of jointing and the formation of composite blocks surrounding

the unstable blocks. The blasting in highly jointed environments in argillaceous and sandstone rock masses are also significantly deleterious. It is evident that the DFN model performed well in determining the height of the blocks formed around the tunnel.

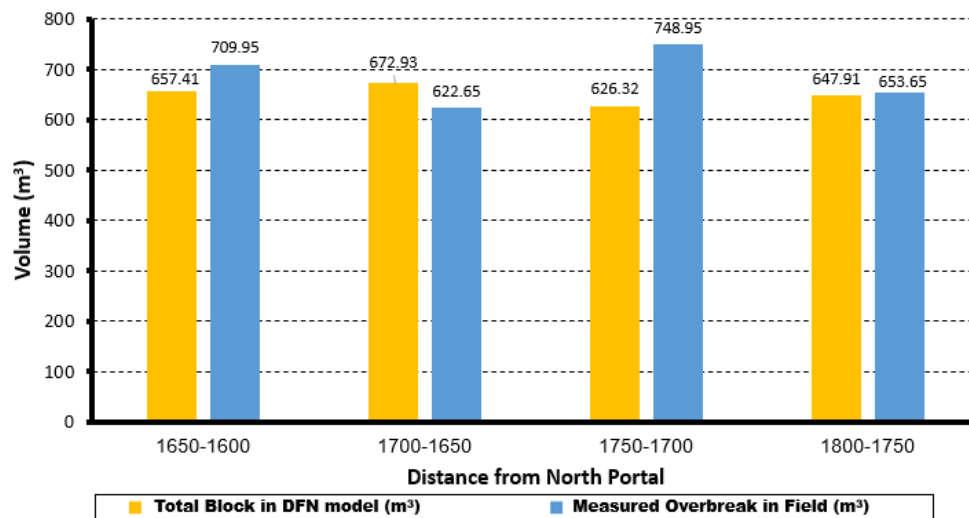


Figure 15. Comparing the total block volume estimated by the DFN model and measured overbreak for each 50 m intervals.

6. Conclusions

In this work, Discrete Fracture Network (DFN) was used to assess the induced overbreak around tunnels based on the geomechanical properties of the rock mass. The geometrical characteristics of discontinuities in 200 meters of the Alborz tunnel, which is located in the Tehran-North freeway in Iran, were surveyed. The DFN model of the studied area was generated. The validity of the DFN model was assessed in terms of orientation distribution of fractures, cumulative distribution of the trace length as well as fracture intensity, and a good agreement was found with field measurements. The average volume of blocks in the studied area was calculated 0.22 m^3 using MDS method. Based on the kinematic stability analysis of blocks around tunnel, the volume of formed blocks prone to instability was estimated 2605 m^3 which showed a good agreement with 2735 m^3 measured overbreak at field. Results of this study showed that utilizing the DFN method provide an appropriate approach for creating a realistic model representing the arrangement of fractures in jointed rock masses. In this method, the interaction between rock blocks can be examined, and ultimately, it can be employed to analyse the stability of jointed rock masses under different conditions. The DFN method can depict blocks around the tunnel susceptible to collapse along with their sizes. Combination of DFN models and discontinuum numerical techniques such as discrete element method serves as a susceptible approach for detailed analysis of excavation damage zones around underground openings.

References

- [1]. Palmstrom, A. & Stille, H. (2007). Ground behaviour and rock engineering tools for underground excavations. *Tunnelling and Underground Space Technology*, 22(4), 363-376.
- [2]. Bahaaddini, M. & Hosseinpour Moghadam, E. (2019). Evaluation of empirical approaches in estimating the deformation modulus of rock masses. *Bulletin of Engineering Geology and Environment*, 78(5), 3493-3507.
- [3]. Bahaaddini, M., Serati, M., Khosravi, M.H. & Hebblewhite, B. (2022). Rock Joint Micro-Scale Surface Roughness Characterisation using Photogrammetry Method. *Journal of Mining and Environment*, 13(1), 87-100.
- [4]. Mohammadi, H.R., Mansouri, H., Bahaaddini, M. & Jalalifar, H. (2017). Investigation into the effect of fault properties on wave transmission. *International Journal for Numerical and Analytical Methods in Geomechanics*, 41(17), 1741-1757.
- [5]. Verma, H.K., Samadhiya, N.K., Singh, M., Goel, R.K. & Singh, P.K. (2018). Blast induced rock mass damage around tunnels. *Tunnelling and Underground Space Technology*, 71, 149-158.
- [6]. Brown, E.T. & Hoek, E. (1980) *Underground Excavations in Rock* (1st ed.), CRC Press, 532 P.
- [7]. Barton, N., Lien, R. & Lunde, J. (1974). Engineering classification of rock masses for the design of tunnel support. *Rock Mechanics and Rock Engineering*, 6(4), 189-236.
- [8]. Foderà, G.M., Voza, A., Barovero, G., Tinti, F. & Boldini, D. (2020). Factors influencing overbreak volumes in drill-and-blast tunnel excavation. A statistical analysis applied to the case study of the

- Brenner Base Tunnel – BBT. *Tunnelling and Underground Space Technology*, 105, 103475.
- [9]. Mahtab, M.A., Rossler, K., Kalamaras, G.S. & Grasso, P. (1997). Assessment of geological overbreak for tunnel design and contractual claims. *International Journal of Rock Mechanics and Mining Sciences*, 34(3), 185.e181-185.e113.
- [10]. Mohammadi, H., Ebrahimi-Farsangi, M.A., Jalalifar, H., Ahmadi, A.R. & Javaheri, A. (2016). Extension of excavation damaged zone due to longwall working effect. *Journal of Mining and Environment*, 7(1), 13-24.
- [11]. Jing, L. & Hudson, J.A. (2002). Numerical methods in rock mechanics. *International Journal of Rock Mechanics & Mining Sciences*, 39(4), 409-427.
- [12]. Singh, S.P. & Xavier, P. (2005). Causes, impact and control of overbreak in underground excavations. *Tunnelling and Underground Space Technology*, 20(1), 63-71.
- [13]. Khalili, S., Monjezi, M., Amini-Khoshalan, H. & Saghat-Foroush, A. (2024). Evaluation the effect of blast pattern on overbreak area around the Miyaneh-Ardabil railway tunnel. *Journal of Mining and Environment*, 15(3), 1149-1160.
- [14]. Farrokh, E., Rostami, J. & Laughton, C. (2012). Study of various models for estimation of penetration rate of hard rock TBMs. *Tunnelling and Underground Space Technology*, 30, 110-123.
- [15]. Innaurato, N., Mancini, R. & Cardu, M. (1998). On the influence of rock mass quality on the quality of blasting work in tunnel driving. *Tunnelling and Underground Space Technology*, 13(1), 81-89.
- [16]. Schmitz, R.M., Viroux, S., Charlier, R. & Hick, S. (2006). The role of rock mechanics in analysing overbreak: application to the Soumagne tunnel. Proc, Eurock 2006: Multiphysics Coupling and Long Term Behaviour in Rock Mechanics. Liège, Belgium, 9-12 May, 631-636.
- [17]. Dey, K. & Murthy, V.M.S.R. (2012). Prediction of blast-induced overbreak from uncontrolled burn-cut blasting in tunnels driven through medium rock class. *Tunnelling and Underground Space Technology*, 28, 49-56.
- [18]. Gong, F.Q., Li, X.B. & Zhang, W. (2008). Over-excavation forecast of underground opening by using Bayes discriminant analysis method. *Journal of Central South University of Technology*, 15(4), 498-502.
- [19]. Jang, H. & Topal, E. (2013). Optimizing overbreak prediction based on geological parameters comparing multiple regression analysis and artificial neural network. *Tunnelling and Underground Space Technology*, 38, 161-169.
- [20]. Daraei, A. & Zare, S. (2018). Prediction of overbreak depth in Ghalaje road tunnel using strength factor. *International Journal of Mining Science and Technology*, 28(4), 679-684.
- [21]. Mottahedi, A., Sereshki, F. & Ataei, M. (2018). Overbreak prediction in underground excavations using hybrid ANFIS-PSO model. *Tunnelling and Underground Space Technology*, 80, 1-9.
- [22]. Dershowitz, W.S. & Einstein, H.H. (1988). Characterizing rock joint geometry with joint system models. *Rock Mechanics and Rock Engineering*. 21(1), 21-51.
- [23]. Hekmatnejad, A., Emery, X. & Elmo, D. (2019). A geostatistical approach to estimating the parameters of a 3D Cox-Boolean discrete fracture network from 1D and 2D sampling observations. *International Journal of Rock Mechanics and Mining Sciences*, 113, 183-190.
- [24]. Dershowitz, W.S. & Herda, H.H. (1992). Interpretation of fracture spacing and intensity. Proc, The 33rd US Symposium on Rock Mechanics (USRMS). Santa Fe, New Mexico, ARMA-92-0757.
- [25]. Staub, I., Fredriksson, A. & Outters, N. (2002). Strategy for a rock mechanics site descriptive model. Development and testing of the theoretical approach. Svensk Kärnbränslehantering AB, Swedish Nuclear Fuel and Waste Management Co. R-02-02.
- [26]. Hadjigeorgiou, J. (2012). Where do the data come from?. *Mining Technology*, 121(4), 236-247.
- [27]. Elmo, D., Rogers, S., Stead, D. & Eberhardt, E. (2014). Discrete Fracture Network approach to characterise rock mass fragmentation and implications for geomechanical upscaling. *Mining Technology*, 123(3), 149-161.
- [28]. Noroozi, M., Kakaie, R. & Jalali, M.E. (2015). 3D stochastic rock fracture modeling related to strike-slip faults. *Journal of Mining and Environment*, 6(6), 169-181.
- [29]. Elmo, D., Stead, D. & Rogers, S. (2015). Guidelines for the quantitative description of discontinuities for use in discrete fracture network modelling. Proc, 13th ISRM International Congress of Rock Mechanics, Montreal, Canada, 10-13 May.
- [30]. Grenon, M., Landry, A., Hadjigeorgiou, J. & Lajoie, P.L. (2017). Discrete fracture network based drift stability at the Éléonore mine. *Mining Technology*, 126(1), 22-33.
- [31]. Noroozi, M., Rafiee, R. & Najafi, M. (2018). Stability analysis of support systems using a coupled FEM-DFN model (Case study: a diversion tunnel at Lorestan dam site, Iran). *Journal of Mining and Environment*, 9(2), 485-497.
- [32]. Rabiei-Vaziri, M., Tavakoli, H. & Bahaaddini, M. (2022). Statistical analysis on the mechanical behaviour of non-persistent jointed rock masses using combined DEM and DFN. *Bulletin of Engineering Geology and Environment*, 81(5), 177.

- [33]. Ghaedi Ghalini, M., Bahaaddini, M. & Amiri Hossaini, M. (2022). Estimation of in-situ block size distribution in jointed rock masses using combined photogrammetry and discrete fracture network. *Journal of Mining and Environment*, 13(1), 175-184.
- [34]. Rogers, S. & Booth, P. (2014). Integrated photogrammetry and DFN modelling for improved rock mass characterisation and engineering design. Proc. 15th Australasian Tunnelling Conference 2014. Carlton South: The Australasian Institute of Mining and Metallurgy, 203–208.
- [35]. General Mechanics Company. (2017). Engineering geology report of eastern tube of Alborz tunnel (north portal) excavation from P.K. 1+600 to 1+800 (Ch. 52+568 to 52+368). GeoData Engineering, Alborz Tunnel.
- [36]. General Mechanics Company. (2017). Excavation Profiles (North portal). GeoData Engineering, Alborz Tunnel.
- [37]. Hammah, R.E. & Curran, J.H. (1998). Fuzzy cluster algorithm for the automatic identification of joint sets. *International Journal of Rock Mechanics and Mining Sciences*, 35(7), 889-905.
- [38]. Pierce, M. (2017). An introduction to random disk discrete fracture network (DFN) for civil and mining engineering applications. *ARMA e-Newsletter*, 20, 3-8.
- [39]. Bonnet, E., Bour, O., Odling, N.E., Davy, P., Main, I., Cowie, P., et al. (2001). Scaling of fracture systems in geological media. *Reviews of Geophysics*, 39(3), 347-383.
- [40]. Davy, P. (1993). On the frequency-length distribution of the San Andreas Fault System. *Journal of Geophysical Research: Solid Earth*, 98(B7), 12141-12151.
- [41]. Priest, S.D. (1993) Discontinuity Analysis for Rock Engineering, Springer.
- [42]. Cottrell, M., Kamera, R. & Hermanson, J. (2017). FracMan kinematic stability assessment of tunnels in Forsmark layout D2. Svensk kärnbränslehantering AB (Swedish Nuclear Fuel and Waste Management). P-15-19.
- [43]. Baecher, G.B., Lanney, N.A. & Einstein, H.H. (1977). Statistical description of rock properties and sampling. Proc. The 18th US Symposium on Rock Mechanics (USRMS). Colorado, USA, 22 June, ARMA-77-0400.
- [44]. Goodman, R.E. & Shi, G. (1985) Block theory and its application to rock engineering. New Jersey: Prentice-Hall, 338 P.



دانشگاه صنعتی شاهرود

نشریه مهندسی معدن و محیط زیست

www.jme.shahroodut.ac.ir: نشانی نشریه:



انجمن مهندسی معدن ایران

ارزیابی اضافه حفاری ایجاد شده در اثر ناپیوستگی‌ها با پیشروی تونل با استفاده از روش شبکه شکستگی مجزا (مطالعه موردی: تونل البرز، ایران)

محمد امین حاجی محمدی^۱، مجتبی بهال‌الدینی^{۱*}، محمد حسین خسروی^۲ و حسن وندیوسفی^۳

۱. دانشکده مهندسی معدن، دانشکده‌گان فنی، دانشگاه تهران، تهران، ایران

۲. بخش مهندسی معدن، دانشکده فنی و مهندسی، دانشگاه بیرجند، بیرجند، ایران

۳. واحد مهندسی ژئوتکنیک، شرکت ژئرال مکانیک، تهران، ایران

چکیده

ناپیوستگی‌ها به عنوان عامل اصلی در بسیاری از ریزش‌های تونل‌ها و فضاهای زیرزمینی شناخته می‌شوند. به منظور جلوگیری از پتانسیل ناپایداری و اضافه حفاری با پیشروی فضای زیرزمینی، لازم است مدلی با توانایی در نظر گرفتن خواص هندسی و مکانیکی ناپیوستگی‌ها تهیه شود. روش شبکه شکستگی مجزا، مدلی واقع‌گرایانه می‌باشد که می‌تواند سیستم پیچیده ناپیوستگی‌ها را نمایش داده و تحلیل نماید. ترکیب مدل شبکه شکستگی مجزا با روش‌های تحلیلی و عددی می‌تواند به عنوان ابزاری علمی برای آنالیز بلوک‌های سنگی ایجاد شده و پایداری آنها تحت شرایط مختلف بارگذاری بکار گرفته شود. هدف از این تحقیق، بررسی اضافه حفاری ایجاد شده با پیشروی تونل البرز واقع در آزادراه تهران-شمال می‌باشد. برای این منظور، در ابتدا خواص هندسی ناپیوستگی‌ها برای ۲۰۰ متر از طول تونل همراه با پیشروی آن برداشت شد. چهار دسته درزه به همراه یک صفحه لایه‌بندی تشخیص داده شد و خواص آماری آن‌ها تعیین گردید. مدل شبکه شکستگی مجزا برای محدوده مطالعاتی تهیه شد و اعتبار آن با مقایسه اطلاعات صحرایی مورد بررسی قرار گرفت. متوسط حجم بلوک در محدوده مطالعاتی ۰/۲۲ متر مکعب تعیین شد. سپس، پایداری بلوک‌های ایجاد شده در اطراف تونل بصورت سینماتیکی مورد بررسی قرار گرفت. حجم بلوک‌های ایجاد شده در اطراف تونل و مستعد ناپایداری تحت بارهای استاتیکی و دینامیکی ۲۶۰۵ مترمکعب تخمین زده شد، در صورتی که مقدار اندازه‌گیری شده آن در منطقه ۲۷۳۵ مترمکعب می‌باشد. همچنین، عمق زون اضافه حفاری تخمین زده شده از طریق مدل ارائه شده در این تحقیق، انطباق مناسبی با اندازه‌گیری برجا نشان داد. نتایج این بررسی نشان می‌دهد که ترکیب روش شبکه شکستگی مجزا با آنالیز پایداری سینماتیکی می‌تواند به عنوان ابزاری مفید و علمی برای بررسی اضافه حفاری ناشی از شرایط زمین‌شناسی در حفاریات زیرزمینی بکار گرفته شود.

اطلاعات مقاله

تاریخ ارسال: ۲۰۲۴/۱۲/۱۷

تاریخ داوری: ۲۰۲۵/۰۲/۲۴

تاریخ پذیرش: ۲۰۲۵/۰۴/۱۰

DOI: 10.22044/jme.2025.15465.2966

کلمات کلیدی

شبکه شکستگی مجزا
پیشروی تونل
اضافه حفاری
تحلیل سینماتیکی
تونل البرز